ISSN 1674-1056
http://cpb.iphy.ac.cn
http://iopscience.iop.org/cpb
中国物理 B
Chinese Physics
中国物理 Chinese Physics B

High efficiency hydrogen purification through P_2C_3 membrane: A theoretical study

Zhao-Qin Chu(储兆琴)[1,2], Xiao Gu(顾晓)[1,2], Xiang-Mei Duan(段香梅)[1,2]
Citation: Chin. Phys. B . 2019, 28(12): 128703 . **doi:** 10.1088/1674-1056/ab55cf
Journal homepage: http://cpb.iphy.ac.cn; http://iopscience.iop.org/cpb

What follows is a list of articles you may be interested in

Electronic properties of size-dependent $MoTe_2$/WTe_2 heterostructure

Jing Liu(刘婧), Ya-Qiang Ma(马亚强), Ya-Wei Dai(戴雅薇), Yang Chen(陈炀), Yi Li(李依), Ya-Nan Tang(唐亚楠), Xian-Qi Dai(戴宪起)
Chin. Phys. B . 2019, 28(10): 107101 . **doi:** 10.1088/1674-1056/ab3b53

First integrals of the axisymmetric shape equation of lipid membranes

Yi-Heng Zhang(张一恒), Zachary McDargh, Zhan-Chun Tu(涂展春)
Chin. Phys. B . 2018, 27(3): 038704 . **doi:** 10.1088/1674-1056/27/3/038704

Combined effects of headgroup charge and tail unsaturation of lipids on lateral organization and diffusion of lipids in model biomembranes

Xiao-Jie Chen(陈晓洁), Qing Liang(梁清)
Chin. Phys. B . 2017, 26(4): 048701 . **doi:** 10.1088/1674-1056/26/4/048701

Application of self-consistent field theory to self-assembled bilayer membranes

Zhang Ping-Wen, Shi An-Chang
Chin. Phys. B . 2015, 24(12): 128707 . **doi:** 10.1088/1674-1056/24/12/128707

Theoretical study of interactions between striated cylindrical particles and membrane

Wang Jing-Jing, Feng Jia-Wei, Ren Chun-Lai
Chin. Phys. B . 2015, 24(8): 088701 . **doi:** 10.1088/1674-1056/24/8/088701

High efficiency hydrogen purification through P_2C_3 membrane: A theoretical study*

Zhao-Qin Chu(储兆琴)[1,2], Xiao Gu(顾晓)[1,2], and Xiang-Mei Duan(段香梅)[1,2,†]

[1] *Department of Physics, Ningbo University, Ningbo* 315211, *China*
[2] *Laboratory of Clean Energy Storage and Conversion, Ningbo University, Ningbo* 315211, *China*

(Received 16 October 2019; published online 29 November 2019)

It is critical to design an effective two-dimensional membrane for hydrogen purification from the mixed gas, due to its wide range of scientific and industrial applications. In this work, we investigate the hydrogen separation performance of P_2C_3 membranes by density functional theory and molecular dynamics simulations. The results show that the energy barrier of the H_2 molecule through the P_2C_3 film is only 0.18 eV, while the energy barriers of the CO, N_2, CO_2, and CH_4 molecules are 0.77 eV, 0.87 eV, 0.52 eV, and 1.75 eV, respectively. In addition, the P_2C_3 film has high H_2 selectivity toward other gas molecules and high H_2 permeability at room temperature. Under 6% tensile strain, 82% hydrogen molecules pass through the film with a H_2 permeance of 2.22×10^7 gas permeance unit (GPU), while other molecules cannot across the membrane at all. Therefore, the P_2C_3 membrane is an excellent material for hydrogen purification.

Keywords: two-dimensional membrane, hydrogen separation, first-principles

PACS: 87.16.D–, 71.15.Mb, 81.05.Rm **DOI:** 10.1088/1674-1056/ab55cf

1. Introduction

It is great important to efficiently separate the light gases (H_2, N_2, CO_2, CO, and CH_4) because most of them are frequently used raw materials in energy, scientific, and chemical fields.[1,2] Under ambient condition, hydrogen is a highly flammable, colorless, transparent, odorless, tasteless, and insoluble gas. Conventional gas separation techniques are complicated to operate and consume a lot of energy, such as cryogenic distillation, pressure swing adsorption polymers, zeolites, and metal–organic frameworks.[3,4] Membrane separation with atomic thickness has emerged, with many advantages, such as suitable pore size to solve permeability and selectivity, high efficiency, ease of operation, and environmental friendliness, soon it has became an ideal candidate for gas separation and caused great interest.[5–10] Since the successful synthesis of graphene in 2004,[11] porous graphene nano-sheets have been widely reported for gas separation due to their extraordinary thermodynamic stability and dynamic stability.[11–13] Jiang *et al.*, using the first-principles density functional theory (DFT) calculations, showed that the designed sub-nanometer porous graphene sheets have high H_2 transmission and high H_2/CH_4 selectivity (about 10^8). Koenig used ultraviolet-induced oxidative etching to produce micrometer-sized graphene films, which could be used as molecular sieves.[14] The experimental results effectively validated the theoretical prediction of porous graphene with gas separation ability. In recent years, to enhance the permeability and selectivity for H_2 and He purification, novel two-dimensional (2D) nanomaterials with various pore sizes have been successively applied to gas separation.[16–20] Still, it is highly desired to develop new 2D membranes with inherently ideal pore sizes for mixed gas separation.

Recently, Chen *et al.*[21] proposed a micrometer-sized monolayer of phosphorus carbide P_2C_3, a porous structure containing P. The pores of this membrane are uniformly distributed, with a diameter of 5.65 Å, which is much larger than the kinetic diameter of H_2 molecule (2.89 Å). Importantly, *ab initio* molecular dynamics (AIMD) simulations showed that, even at temperature up to 1100 K, the P_2C_3 sheet retains its structural integrity and has no soft mode, indicating remarkable thermal stability. It can be expected that the P_2C_3 film could exhibit good H_2 separation performance.

In this work, we investigate the H_2 separation performance of the P_2C_3 monolayer based on the DFT and AIMD simulations. The results show that the stability of the porous P_2C_3 monolayer is sufficiently high to be used as a separation membrane. The energy barrier for the considered gas molecules passing through P_2C_3 membrane is clearly divided into two camps, the barrier of H_2 is lower than 0.2 eV, while the values of CO, N_2, CO_2, and CH_4 are all above 0.5 eV. To further estimate the H_2 separation performance of the P_2C_3 sheet, the gas selectivity and H_2 permeance are analyzed.

2. Calculation methods

Our calculations were carried out using the Vienna *ab initio* simulation package (VASP).[22,23] The exchange–

*Project supported by the National Natural Science Foundation of China (Grant Nos. 11574167 and 11874033) and the KC Wong Magna Foundation in Ningbo University, China.

†Corresponding author. E-mail: duanxiangmei@nbu.edu.cn

© 2019 Chinese Physical Society and IOP Publishing Ltd

correlation interactions were described by a generalized gradient approximation (GGA)[24] with the Perdew–Burke–Ernzerhof (PBE) functional.[25] A damped van der Waals correction in Grimme's scheme (DFT + D2)[26] was included in all the calculations. The cut-off energy for plane waves was set at 500 eV, and the convergence criteria for force and energy on each atom during structure relaxation were set to 0.005 eV·Å^{-1} and 10^{-5} eV, respectively. To avoid the interaction between the neighboring periodic structures, we adopted periodic boundary conditions with a vacuum space of 20 Å. The climbing image nudged elastic band (CINEB) was used to search the transition state (TS) when gas diffused through the pores. The 2 ×2 unit cell of P_2C_3 was used as the model for CINEB calculations. The Brillouin zone was sampled with the Monkhorst–Pack k-mesh of $5 \times 5 \times 1$ in reciprocal space during the geometry optimization and dynamics. MD simulations were performed in the canonical ensemble (NVT) using Nosé–Hoover thermostat to control the temperature.[27] The condensed-phase optimized molecular potential for atomistic simulation studies (COMPASS) force-field was used to performance the atomic interactions. The atom-based van der Waals interactions and Ewald electrostatic interaction were set with a cutoff distance of 12.5 Å. Every simulation ran for 5 ns with a time step of 1.0 fs.

3. Results and discussion

3.1. The optimized geometry and cohesive energy of P_2C_3

The optimized geometry of P_2C_3 is shown in Fig. 1(a). A P_2C_3 structure of 2×2 supercell is optimized by DFT calculations. The diameter of the pore is 5.65 Å and the C–P bond length is 1.63 Å, which are in good agreement with the previous studies, where the diameter of the pore and the bond-length are 5.69 Å and 1.64 Å, respectively.[21] The size of the pore is suitable for a molecule sieve, which is much larger than that of graphene (2.46 Å)[28] and silicene (3.87 Å).[29] The cohesive energy is calculated as

$$E_{\text{coh}} = (n_{\text{C}}E_{\text{C}} + n_{\text{P}}E_{\text{P}} - E_{\text{tot}})/(n_{\text{C}} + n_{\text{P}}), \quad (1)$$

where E_{C}, E_{P}, and E_{tot} are the energies of isolated C atom, P atom, and the total energy of the P_2C_3 membrane, respectively, n_{C} and n_{P} are the corresponding numbers of C and P atoms. The calculated cohesive energy of the P_2C_3 sheet is 4.66 eV/atom, higher than 3.71 eV/atom of silicene,[30] and the latter has been reported to be stable enough for gas separation.[31]

During the experimental process, strain is unavoidable. Tensile strain would increase the pore size and reduce the cohesive energy. In Fig. 1(b), we show how the cohesive energy varies with tensile strain. It is reasonable that E_{coh} is reduced as the strain increases. At 10% strain, the cohesive energy is still greater than 4.1 eV. Therefore, the P_2C_3 membrane should be safely utilized for hydrogen separation.

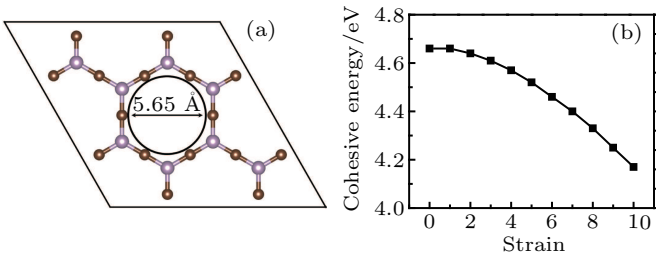


Fig. 1. (a) The optimized P_2C_3 structure of 2×2 supercell. Pink and brown balls represent phosphorus and carbon atoms, respectively. (b) The cohesive energy of P_2C_3 as a function of the tensile strain.

3.2. The energy barrier of the gas molecules

Using the CINEB method, we calculate the energy barrier of the gas molecules passing through the pores, which is defined as

$$E_{\text{b}} = E_{\text{TS}} - E_{\text{SS}}, \quad (2)$$

where E_{TS} and E_{SS} are the total energies of the system when a gas molecule is adsorbed on the P_2C_3 membrane at the transition states (TS) and at the most stable states (SS), respectively. Figure 2 shows the minimum energy pathways for the considered gas molecules passing through the P_2C_3 sheet. Note that the energy barrier for H_2 molecule passing through the membrane is only 0.18 eV, which is much lower than that for CO (0.77 eV), N_2 (0.87 eV), CO_2 (0.52 eV), and CH_4 molecules (1.75 eV). Obviously, using the P_2C_3 membrane as a molecular sieve, it is easy to separate hydrogen from other gases in one step. In addition, the CO_2 molecule has two saddle points, while the other gas molecules have only one. The main reason is that O–C–O (close to the pore) in the CO_2 molecule is charged negatively, positively, and negatively, respectively. When the first O atom of the CO_2 approaches the cavity, the repulsive force between it and the film becomes weak as the adsorption height decreases.

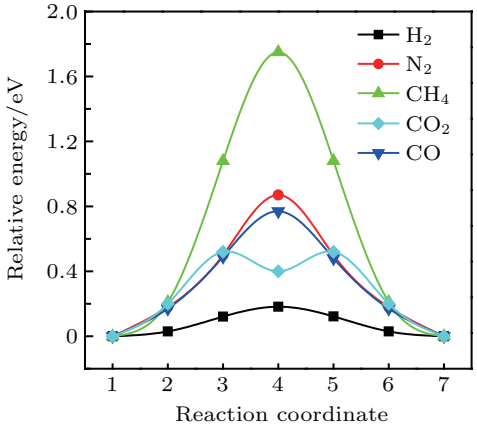


Fig. 2. The minimum energy pathways for gas molecules passing through P_2C_3 membrane.

In Table 1, we list the kinetic diameter (D) and the energy barrier (E_{b}) of the gas molecules passing through the film. The

general trend is that as the kinetic diameter becomes larger, the energy barrier of the molecule generally increases. The electron density isosurface of the system as molecules H_2 and CH_4 pass through the membrane is shown in Fig. 3. It can be intuitively seen that as the dynamic diameter of the gas molecules becomes larger, the electron density overlap between the gas molecule and the film increases, and thus the barrier of the molecules raises. For the H_2 molecule, there is no electron overlap between it and the P_2C_3 film, so it can easily cross the film with the lowest energy barrier. The electron overlap between the film and the CH_4 molecule is the largest, and the energy barrier is also the highest.

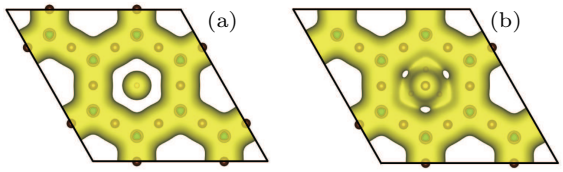


Fig. 3. Electron density isosurfaces when (a) H_2 and (b) CH_4 molecules passing through P_2C_3 membrane. The isovalue is set to be 0.015 e/Å^3.

Table 1. The kinetic diameter D and the energy barrier E_b of the molecule passing through the P_2C_3 membrane.

	H_2	CO	CO_2	N_2	CH_4
D/Å	1.80	3.76	3.30	3.64	3.80
E_b/eV	0.18	0.77	0.52	0.87	1.75

3.3. The selectivity and permeability

With the energy barrier E_b, we use the Arrhenius equation[32] to calculate the selectivity of H_2 relative to other gas molecules, which can be given as

$$S_{H_2/gas} = \frac{r_{H_2}}{r_{gas}} = \frac{A_{H_2}\exp(-E_{H_2}/RT)}{A_{gas}\exp(-E_{gas}/RT)}, \quad (3)$$

where A is the diffusion prefactor and is usually taken as a constant[33] of 10^{11} s^{-1}, and r is the diffusion rate of gas molecules. As the kinetic energy becomes larger, the diffusion rate of gas molecules increases significantly with temperature (see Fig. 4(a)). It is worth noting that the H_2 molecule has the highest diffusion rate due to its lowest energy barrier. In addition, the selectivity of hydrogen decreases with increasing temperature (see Fig. 4(b)). This is easy to understand because the kinetic energy of the gas molecules increases effectively with temperature, thereby reducing the impact of the energy barrier. The selectivity of H_2 relative to CO_2, CO, N_2, CH_4 at room temperature is 3.5×10^5, 5.5×10^9, 2.6×10^{11}, 1.6×10^{26}, respectively. The H_2 selectivity of the P_2C_3 film is much higher than the standard for industrial applications.[34] Importantly, it takes only one step to completely separate H_2 from other gases.

Permeability is another important criterion for evaluating the H_2 separation performance of the P_2C_3 sheet. We investigate whether mixed gas molecules (composed of 72 H_2, 36 CO, 36 CO_2, 36 CH_4, 36 N_2 molecules) at room temperature can pass through the film. The permeability can be obtained by

$$F = \frac{n}{S\times t\times\Delta p}, \quad (4)$$

where t, S, and n represent the time duration, the area (33.90 Å×33.90 Å) of the P_2C_3 membrane, and the numbers of gas molecules in the permeate side, respectively. And the pressure drop Δp is set to 1×10^5 Pa when the mixed gas molecules pass though the hole. The process can be divided into three steps. First, the mixed gas molecules approach the membrane under the van der Waals interaction. Part of them then pause for a few picoseconds on the surface of P_2C_3. In the end, due to the gas pressure difference between two sides of the membrane, some gas molecules across the P_2C_3 membrane, reach the other side, and diffuse into the vacuum. The configurations of the system, after running the MD simulation at room temperatures for 5 ns, are shown in Fig. 5(a). It turns out that only H_2 can penetrate the P_2C_3 membrane while other gas molecules cannot at the considered temperatures. There are 56 hydrogen molecules on the other side of the membrane (the initial number is 72), and the passing through ratio is as high as 78%. Particularly, the H_2 permeance at room temperature is calculated to be 2.01×10^7 gas permeance unit (GPU), which is much higher than the industrially accepted standard (20 GPU) for gas separation.[34] Therefore, we predict that the porous P_2C_3 membrane should be applicable for hydrogen purification with extremely high selectivity and permeance.

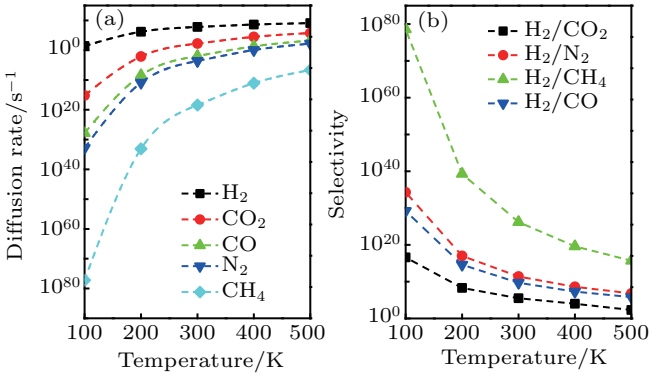


Fig. 4. (a) Diffusion rates of all the studied gas molecules (H_2, CO, CO_2, N_2, CH_4) and (b) H_2 selectivity relative to other gas molecules as a function of temperature.

The penetration rate of hydrogen gas can be further increased by increasing the size of the molecular sieve by mechanical strain. We consider the different tensile strains and find that applying 6% strain to the membrane not only improves the H_2 pass rate (the penetration of H_2 can reach 2.22×10^7 GPU), but also successfully prevents other molecules from passing through. Under the 8% strain, the carbon dioxide molecules begin to pass through the membrane (see Fig. 5(b)), which can no longer be used to purify hydrogen. To effectively

separate hydrogen from the mixed gas, the 6% stretched P_2C_3 membrane is the best choice as a molecular sieve.

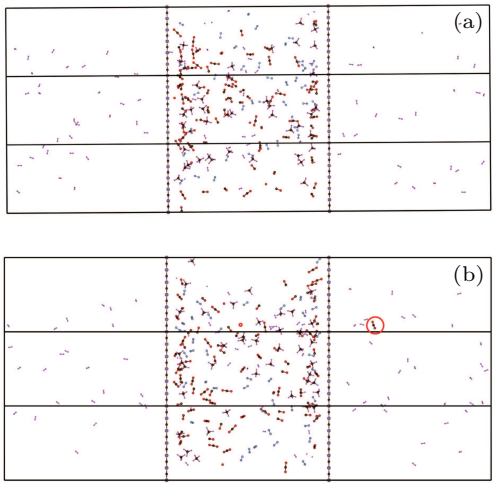


Fig. 5. The snapshot of MD simulations for the gas mixture permeating through (a) the pristine P_2C_3 membrane and (b) the 8% stretched membrane at 300 K.

4. Conclusion

Based on DFT and MD simulations, we investigate the diffusion and selectivity of hydrogen, carbon monoxide, nitrogen, carbon dioxide, and methane through a porous P_2C_3 film. The results show that the energy barrier of hydrogen passing through the membrane is as low as 0.18 eV, while the values of other molecules are higher than 0.5 eV, which indicates that hydrogen and other gases can be effectively separated in one step. At room temperature, the P_2C_3 membrane has a very high H_2 permeability, when the mechanical strain increases to 6%, the permeability can reach 2.22×10^7 GPU. We predict that the P_2C_3 membrane is an excellent material for hydrogen purification in terms of H_2 selectivity and permeability.

References

[1] Keskin S, van Heest T M and Sholl David S 2010 *Chem. Sus. Chem.* **3** 879
[2] Yuan Y, Sun F X, Li L, Cui P and Zhu G S 2014 *Nat. Commun.* **5** 4260
[3] Hall H E, Ford P J and Thompson K 1966 *Cryogenics* **6** 80
[4] Das N K, Chaudhuri H, Bhandari R K, Ghose D and Sen P 2008 *Curr. Sci.* **6** 1684
[5] Shan M X, Xue Q Z, Jing N N, Ling C C and Zhang 2012 *Nanoscale* **4** 5477
[6] Hu W, Wu X J, Li Z Y and Yang J L 2014 *Phys. Chem. Chem. Phys.* **16** 6957
[7] Gao G P, Jiao Y, Ma F X, Jiao Y L, Kou L Z, Waclawik E and Du A J 2017 *Int. J. Hydrogen Energ.* **42** 5577
[8] Chang X X, Qing Z, He D, Zhu L, Li X F and Tao B S 2017 *Int. J. Hydrogen Energ.* **42** 24189
[9] Jiao Y, Du A J, Smith Sean C, Zhu Z H and Qiao S Z 2015 *J. Mater. Chem. A* **3** 6767
[10] Jiao Y, Du A J, Hankel M, Zhu Z H, Rudolph V and Smith S C 2011 *Chem. Commun.* **47** 11843
[11] Novoselov K S, Geim A K, Morozov S V and Jiang D 2004 *Science* **306** 666
[12] Jiang D E, Cooper, Valentino R and Dai S 2009 *Nano. Lett.* **9** 4019
[13] Liu H J, Chen Z F, Dai S and Jiang D E 2015 *J. Solid State Chem.* **224** 2
[14] Liu H J, Dai S and Jiang D E 2013 *Solid State Commun.* **175** 101
[15] Koenig S P, Wang L D, Pellegrino J and Bunch J S 2012 *Nat. Nanotechol.* **7** 728
[16] Ma Z N, Zhao X D, Tang Q and Zhou Z 2014 *Int. J. Hydrogen Energ.* **39** 5037
[17] Bartolomei M, Carmona N, Estela and Hernández M I 2014 *J. Phys. Chem. C* **118** 29966
[18] Cranford S W and Buehler M J 2012 *Nanoscale* **4** 4587
[19] Zhang H Y, He X J, Zhao M W, Zhang M, Zhao L X, Feng X J and Luo Y H 2012 *J. Phys. Chem. C* **116** 16634
[20] Rao Y C and Chu Z Q, Gu X and Duan X M 2019 *Comput. Mater. Sci.* **161** 53
[21] Huang S L, Xie Y E, Zhong C Y and Chen Y P 2018 *J. Phys. Chem. Lett.* **9** 2751
[22] Kresse G and Furthmüller J 1996 *Comput. Mater. Sci.* **6** 15
[23] Kresse G and Furthmüller J 1996 *Phys. Rev. B* **54** 11169
[24] Perdew J P, Ernzerhof M and Burke K 1996 *Phys. Rev. Lett.* **77** 3865
[25] Perdew J P, Ernzerhof M and Burke K 1996 *J. Chem. Phys.* **105** 9982
[26] Grimme S 2006 *J. Comput. Chem.* **27** 1787
[27] Wu T T, Xue Q Z, Ling C C, Shan M X, Liu Z L, Tao Y H and Li X F 2014 *J. Phys. Chem. C* **118** 7369
[28] Min H K, Sahu, Bhagawan, Banerjee, Sanjay K and MacDonald A H 2007 *Phys. Rev. B* **75** 155115
[29] Ni Z Y, Liu Q H, Tang K C, *et al.* 2011 *Nano. Lett.* **12** 113
[30] Li Y F, Liao Y L and Chen Z F 2014 *Angew. Chem. Int. Edit.* **53** 7248
[31] Hu W, Wu X J, Li Z Y and Yang J L 2013 *Nanoscale* **5** 9062
[32] Arrhenius S 1889 *Zeit. Phys. Chem.* **4** 226
[33] Blankenburg S, Bieri M, Fasel R, Müllen K, Pignedoli C A and Passerone D 2010 *Small* **6** 2266
[34] Zhu Z Q 2006 *J. Membr. Sci.* **281** 754